INTERNATIONAL JOURNAL OF
RADIATION ONCOLOGY • BIOLOGY • PHYSICS
www.redjournal.org

CLINICAL INVESTIGATION

Association of Multi-Kingdom Skin Microbiota With Radiation Dermatitis in Patients With Breast Cancer After Reconstructive Surgery: A Prospective, Longitudinal Study

Wei Shi, MD, PhD,[a,b,c,d] Li Zhang, MD, PhD,[a,b,c,d] Zhiming Li, PhD,[e] Xu Zhao, MD, PhD,[a,b,c,d] Wailok Lui, MD, PhD,[a,b,c,d] Jin Meng, MD, PhD,[a,b,c,d] Xingxing Chen, MD, PhD,[a,b,c,d] Xin Mei, MD, PhD,[a,b,c,d] Jinli Ma, MD, PhD,[a,b,c,d] Zhaozhi Yang, MD, PhD,[a,b,c,d] Jingjing Xia, MD, PhD,[f] Jiucun Wang, PhD,[e,g] Zhen Zhang, MD, PhD,[a,b,c,d] Zhimin Shao, MD, PhD,[b,h] Xiaoli Yu, MD, PhD,[a,b,c,d] and Xiaomao Guo, MD, PhD[a,b,c,d]

[a]Department of Radiation Oncology, Fudan University Shanghai Cancer Center, Shanghai, China; [b]Department of Oncology, Shanghai Medical College, Fudan University, Shanghai, China; [c]Shanghai Clinical Research Center for Radiation Oncology, Shanghai, China; [d]Shanghai Key Laboratory of Radiation Oncology, Shanghai, China; [e]State Key Laboratory of Genetics and Development of Complex Phenotypes, Fudan University, Shanghai, China; [f]Greater Bay Area Institute of Precision Medicine (Guangzhou), School of Life Sciences, Fudan University, Guangzhou, China; [g]Research Unit of Dissecting the Population Genetics and Developing New Technologies for Treatment and Prevention of Skin Phenotypes and Dermatological Diseases (2019RU058), Chinese Academy of Medical Sciences, Shanghai, China; and [h]Department of Breast Surgery, Fudan University Shanghai Cancer Center, Shanghai, China

Received Jan 2, 2025; Revised Mar 14, 2025; Accepted for publication Mar 26, 2025

Background: The clinical significance of multi-kingdom skin microbiota in acute radiation dermatitis (ARD) is not well understood. We hypothesized that skin microbiota is associated with ARD in patients with breast cancer (BC) undergoing radiation therapy (RT) after reconstructive surgery.

Methods and Materials: A total of 412 skin microbiota samples from 103 patients, taken before and after RT, from both the treated and contralateral healthy sides, were analyzed using bacterial 16S ribosomal RNA (rRNA) V3-V4 region and fungal rRNA internal transcribed spacer (ITS) sequencing. ARD was graded using the Toxicity Criteria of the Radiation Therapy Oncology Group (RTOG). Patients were divided into 2 groups: no or mild ARD subgroup (N_MD, RTOG grade 0-1) and significant ARD subgroup (SD, RTOG grade $\geq$ 2).

Results: Significant differences in skin microbiota were observed between the N_MD and SD subgroups, with *Staphylococcus*, *Cutibacterium*, and *Malassezia* genera enriched in SD and *Ralstonia* and *Methyloversatilis* enriched in N_MD. Network

Corresponding authors: Xiaomao Guo, MD, PhD; Xiaoli Yu, MD, PhD; E-mail: stephanieyxl@hotmail.com, guoxm1800@126.com

Wei Shi, Li Zhang, Zhiming Li, and Xu Zhao made equal contributions to this study.

This protocol is registered with ClinicalTrials.gov Identifier, NCT05032768.

Author Responsible for Statistical Analysis: Wei Shi and Zhiming Li.

Disclosures: none.

This work was supported by the National Natural Science Foundation of China (grant numbers 82003257, 82102829, 81972846, 82003231), Shanghai Cancer Prevention and Treatment Development Foundation (CYBER-2021-002), Noncommunicable Chronic Diseases-National Science and Technology Major Project (2023ZD0502200), CAMS Innovation Fund for Medical Sciences (2019-I2M-5-066) and Shanghai Municipal Science and Technology Major Project (2023SHZDZX02).

Data Sharing Statement: All sequencing results were deposited in NODE (The National Omics Data Encyclopedia) (https://www.biosino.org/node) under project ID PRJCA024773 and PRJCA025087. The authors declare that all data supporting the findings of this study are available within the paper or from the corresponding authors upon request.

Acknowledgments —We thank the Fudan University Shanghai Cancer Center for its support and all the participants who volunteered for this study.

Supplementary material associated with this article can be found in the online version at doi:10.1016/j.ijrobp.2025.03.077.

Int J Radiation Oncol Biol Phys, Vol. 123, No. 1, pp. 161–170, 2025

https://doi.org/10.1016/j.ijrobp.2025.03.077

analysis revealed that interkingdom and intrakingdom ecological interactions were more notable and stable in N_MD than SD over the course of RT. Importantly, 2 dermotypes with robust patterns of microbial networks were identified, with the "D-dermotype" (highly diversified and dominated by *Devosiaceae*) composing entirely of N_MD. Dermatitis-prediction classifiers were constructed. Classifiers I and III, which included bacterial variables with or without fungal variables, performed significantly better than classifier II, which relied solely on fungal variables. Bacteria-based classifier I yielded the best area under the curve in the test set of 94.64% (95% confidence interval, 83.58%-100%).

Conclusions: This prospective longitudinal study indicated an association between multi-kingdom skin microbiota and the development of significant ARD in patients with BC undergoing RT after reconstructive surgery, implying the possible application of skin microbiota in the prediction of ARD and microbial therapy in the management of ARD.

Introduction

Human skin harbors millions of microorganisms (including bacteria and fungi) that comprise the skin microbiota, an intricate and dynamic multi-kingdom ecosystem. Skin microbiota is characterized by significant individual uniqueness and local biogeography. Dysbiosis of skin microbiota has been increasingly implicated in many skin diseases.[1,2]

Radiation therapy (RT) is an important treatment modality for breast cancer (BC). Approximately 95% of patients treated with RT experience varying degrees of acute radiation dermatitis (ARD).[3] After reconstructive surgery, patients will have impaired skin thermoregulatory reflexes and greater skin stretching, therefore they may experience an increased risk and severity of ARD.[4] ARD can cause pain, itching, and burning, greatly affecting the quality of life and aesthetics of patients. Severe ARD can lead to treatment interruption or delay.[3] In patients with BC who have undergone reconstructive surgery, ARD is a significant concern because it may increase the risk of infection and delayed wound healing, thereby raising the likelihood of reconstruction failure.[5] Owing to progress in RT technology [eg, intensity-modulated radiation therapy (IMRT)], the incidence of ARD has been markedly decreased. Nevertheless, even mild ARD can significantly affect quality of life and self-image, which are of great concern for the patients after reconstructive surgery. The pathogenesis of ARD remains unclear and recommendations for its prevention and treatment are limited.[6]

Recent studies that recruited patients with different cancer types reported a relationship between skin bacterial microbiota and the occurrence and healing rate of ARD.[7-10] Furthermore, clinical trials demonstrated that bacterial decolonization may be effective in the prevention of ARD.[11,12] As the skin microbiota is shaped by the physiological characteristics of different body parts, studies that included patients with different cancer types have the confounding factor of differential skin microbiota communities in different body parts; therefore, the effects of RT on skin microbiota cannot be fully elucidated. In addition, research has yet to unravel the association of skin multi-kingdom (both bacterial and fungal microbiota) ecological networks before and after RT with ARD. Here, we report the results from, to our knowledge, the first prospective, longitudinal trial analyzing the interaction of multi-kingdom skin microbiota with ARD in patients with BC undergoing RT after reconstructive surgery.

Methods and Materials

Study design and study participants

One hundred and three patients were prospectively enrolled between January 2021 and September 2022 at an academic cancer center (NCT05032768). Eligible patients were adults aged 18 to 70 years with BC after autologous and/or implant reconstructive surgery, and plans for adjuvant RT. Patients were excluded if they received chemotherapy, antibiotics, steroids, or immunosuppressants within 4 weeks before skin microbiota sampling. Cleansing with antibacterial cleansers was not permitted within 7 days before sample collection. No bathing, shampooing, or moisturization was allowed within 24 hours of sample collection. For each of the enrolled patients, skin microbiota samples were sequentially collected on the initial day and 1 day after completion of RT from both the treated and contralateral healthy sides of the patients.

The primary outcome was the association of skin microbiota with the development of grade 2 or higher ARD. Patients' skin reactions were graded by investigators (W.S. and L.Z.) blinded to microbiome information using the modified version of Toxicity Criteria of the Radiation Therapy Oncology Group (RTOG)[13] weekly during RT, weekly up to 6 weeks after RT, and at 3, 6, 9, 12, and 24 months after RT. The worst scores during RT and up to 3 months after RT were chosen. Patients were divided into 2 groups: no or mild ARD subgroup (N_MD, RTOG grade 0-1) and significant ARD subgroup (SD, RTOG grade $\geq$ 2). This study was approved by the Institutional Ethics Committee (2104234-7). Written informed consent was obtained from all patients.

Skin microbiota sampling and DNA extraction

To obtain sufficient DNA from skin sites, a skin area of 4 cm^2 was swabbed with sterile polyester fiber-headed swabs

moistened with a solution of 0.15 M NaCl. The sampling region was swabbed 40 times. Negative controls of mock swabs were collected and analyzed for each sampling. DNA was extracted using the cetyltrimethylammonium bromide method. DNA was quantified using Qubit (Invitrogen).

Polymerase chain reaction amplification and sequencing

The bacterial 16S ribosomal RNA (rRNA) V3-V4 region and fungal internal transcribed spacer (ITS) region were amplified using the universal primers 341F/805R and ITS1FI2/ITS2, respectively, for library construction. The polymerase chain reaction (PCR) amplification conditions were as follows: 32 cycles of pre-denaturation at 98°C for 30 seconds, denaturation at 98°C for 10 seconds, annealing at 54°C for 30 seconds, and extension at 72°C for 45 seconds. The final extension step was performed at 72°C for 10 min. PCR products were purified using AMPure XT Beads (Beckman Coulter Genomics) and quantified using Qubit (Invitrogen). The purified PCR products were evaluated using an Agilent 2100 Bioanalyzer (Agilent) and Illumina library quantitative kits (Kapa Biosciences), which were pooled and sequenced on an Illumina NovaSeq 6000 (PE250) provided by LC-Bio Technology Co., Ltd.

Sequence processing and bioinformatic analysis

Sequencing primers were removed from the demultiplexed raw sequences using Cutadapt (v1.9) (RRID:SCR_011841).[14] Paired-end reads were merged using FLASH (v1.2.8).[15] Low-quality reads (quality scores < 20), short reads (<100 bp), and reads containing more than 5% "N" records were trimmed using the sliding-window algorithm in fqtrim (v 0.94). Quality filtering was performed to obtain high-quality clean tags according to the fqtrim. Chimeric sequences were filtered using Vsearch software (v2.3.4). DADA2 was used to denoise and generate amplicon sequence variants. Sequence alignment of species annotations was performed using the QIIME2 plugin feature classifier, and the alignment databases used were SILVA and NT-16S. Samples with a sequencing depth <40,000 reads were removed.

Alpha and beta diversities were calculated using the QIIME2. To identify differentially enriched taxa between the groups, high-dimensional class comparisons via linear discriminant analysis effect size (LEfSe)[16] were used. The microbial co-occurrence networks were inferred using Spearman's rank correlations and visualized using OmicStudio tools at https://www.omicstudio.cn/tool, with a Spearman rho $\geq$ 0.5 and $P < .05$, respectively. To predict metagenomic functional content, Phylogenetic Investigation of Communities by Reconstruction of Unobserved States (PICRUSt2) was performed.[17] Pathways were predicted using the MetaCyc database (RRID:SCR_007778).[18]

The determination of skin microbial dermotypes

Skin microbiome types were defined as described in a previous study.[19] All the samples were clustered using the Jensen−Shannon distance. Clustering was performed around the medoid (PAM) using the PAM function in the cluster[20] package in R. The optimal number of clusters was determined using the Calinski−Harabasz index. Principal coordinates analysis (PCoA) was used to display the dermotype results using the cmdscale function in R. The dermotype results were also subjected to a PERMANOVA test based on the Bray−Curtis (BC) distance using the vegan package (RRID:SCR_011950).[21]

Establishment of dermatitis-prediction classifier

To establish microbial classifiers associated with the severity of ARD, we utilized the random forest algorithm to analyze microbial variables in skin samples. Initially, microbial taxa significantly associated with the degree of ARD were identified through differential analysis and were selected as input variables for the model. The sample data were randomly split into a training set and a test set at an 80% to 20% ratio. All microbial data were standardized before modeling to mitigate the impact of varying data scales. The random forest model was implemented using the randomForest package in R (RRID:SCR_015718).[22] The model parameters were set as follows: importance = TRUE, proximity = TRUE, and ntree = 1000. After training, the model was internally validated using the training set and externally validated using a 20% test set to assess its predictive performance. The performance of the model was evaluated by calculating the area under the curve (AUC) and using the receiver operating characteristic (ROC) curve to analyze the sensitivity and specificity of the model.

Additionally, mean decrease accuracy (MDA) was calculated to evaluate the importance of each microbial variable in the model. This was achieved by permuting the values of each variable in the test set one at a time and measuring the decrease in model accuracy. MDA scores were derived by averaging the decreases in accuracy across all permutations, providing a quantitative measure of the impact of each variable on model performance. This analysis helps identify the microbes that are most influential in predicting the severity of ARD.

Statistical analysis

Continuous data were analyzed using the Wilcoxon rank-sum test and categorical data were analyzed using Pearson's χ^2 test or Fisher's exact test. All statistical analyses were conducted using R software, and a 2-sided $P < .05$ was considered statistically significant.

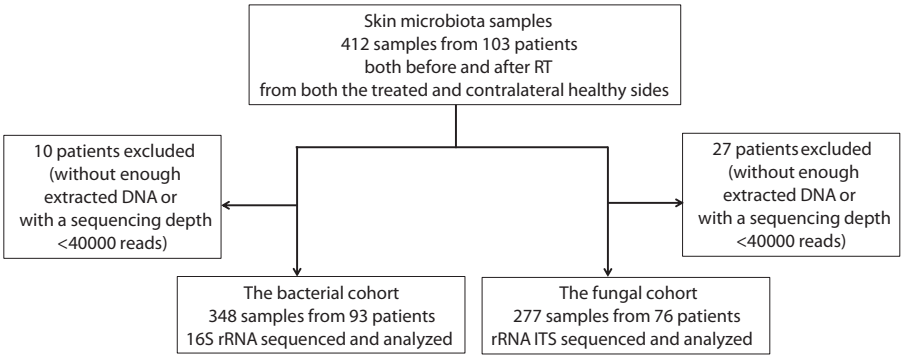

Fig. 1. Flow diagram of sample processing.

Results

Patient characteristics and overall skin microbiota profile

A total of 412 skin microbiota samples were collected from 103 patients, both before and after RT, from both treated and contralateral healthy sides. After excluding samples without sufficient DNA, skin microbiota samples from 93 patients in the bacterial cohort and 76 patients in the fungal cohort were analyzed (Fig. 1). The primary outcome was the association of skin microbiota with the development of grade 2 or higher ARD. Patients were divided into 2 groups: no or mild ARD subgroup (N_MD, RTOG grade 0-1) and significant ARD subgroup (SD, RTOG grade ≥ 2).

The baseline demographic and clinical characteristics of the patients are shown in Table 1. Overall, all patients were classified as type 4 on the Fitzpatrick skin scale.[23] In the bacterial cohort, N_MD consisted of 69 patients (74.2%; grade 0: 1 patient; grade 1: 68 patients) and SD consisted of 24 patients (25.8%; grade 2: 21 patients; grade 2.5: 1 patient; grade 3: 2

Table 1 Demographic and clinical characteristics of patients by severity of acute radiation dermatitis

Characteristic	Bacterial cohort (N = 93)			Fungal cohort (N = 76)		
	N_MD	SD	*P* value	N_MD	SD	*P* value
Age, y	(N = 69)	(N = 24)		(N = 59)	(N = 17)	
<40	39	16	.384	33	12	.279
≥40	30	8		26	5	
BMI (kg/m^2)						
<24	54	21	.492	46	15	.554
≥24	15	3		13	2	
PTV volume of reconstructed chest wall (cm^3), medium (range)	780 (441-1304)	750 (561-1115)	.652	768 (504-1304)	770 (561-1115)	.906
Menopausal status						
Premenopausal	62	22	1.000	54	15	1.000
Postmenopausal	7	2		5	2	
Reconstruction type						
Autologous ± implant reconstruction	24	9	.811	19	7	.492
Implant reconstruction	45	15		40	10	
Anti-HER2 therapy						
Yes	22	3	.065	17	2	.266
No	47	21		42	15	
Chemotherapy						
Neoadjuvant	15	6	.742	12	6	.340
Adjuvant ± neoadjuvant	54	18		47	11	

Abbreviations: BMI = body mass index; PTV = planning target volume.

patient). In the fungal cohort, N_MD consisted of 59 patients (77.6%; grade 0: 1 patient; grade 1: 58 patients), and SD consisted of 17 patients (22.4%; grade 2: 16 patients; grade 3: 1 patient). Two patients in the bacterial cohort and 1 patient in the fungal cohort experienced severe radiodermatitis (RTOG grade 3), marked by confluent moist desquamation. Most patients were under 40 years of age, had a body mass index (BMI) of less than 24 kg/m^2, were in a premenopausal state, and underwent implant-based reconstruction. IMRT was used. All patients received a prescribed dose of 50 Gy/25 fractions over 5 weeks. A 3-mm tissue-equivalent bolus was applied for 15 fractions. Notably, patients in the N_MD and SD subgroups were similar with respect to age, BMI, breast size measured by planning target volume of reconstructed chest wall, menopausal status, reconstruction type, and systemic therapy (Table 1). We first assessed the landscape of skin microbiota in patients with BC undergoing RT after reconstructive surgery via bacterial 16S rRNA V3-V4 region and fungal ITS sequencing, noting that communities were relatively diverse, with a high abundance of *Proteobacteria* and *Basidiomycota* phyla in the skin microbiota (Fig. 2A).

The skin microbial dermotypes and skin microbiota variations over the course of RT

We compared the skin microbiota before and after RT to investigate the impact of RT on the skin microbial community in patients with BC and whether these perturbations in the skin microbiota would correlate with the severity of ARD. We analyzed the richness and diversity of the skin microbiota before and after RT, and no significant differences were observed (Fig. E1A, B), suggesting that RT does not induce dramatic changes in the overall structure of the skin microbiota community. The PCoA based on Bray−Curtis dissimilarity metrics showed some but not dramatic differences according to sampling time points (Fig. E1C, D).

A previous study indicated that 2 distinct cutaneous microbial typologies were present in the skin that are significantly associated with skin phenotypes.[19] Consequently, we classified the skin according to the previously reported typologies. All skin microbiota samples (n = 140: 68 before RT and n = 72 after RT) formed 2 separate clusters, representing 2 skin types. We defined these 2 dermotypes based

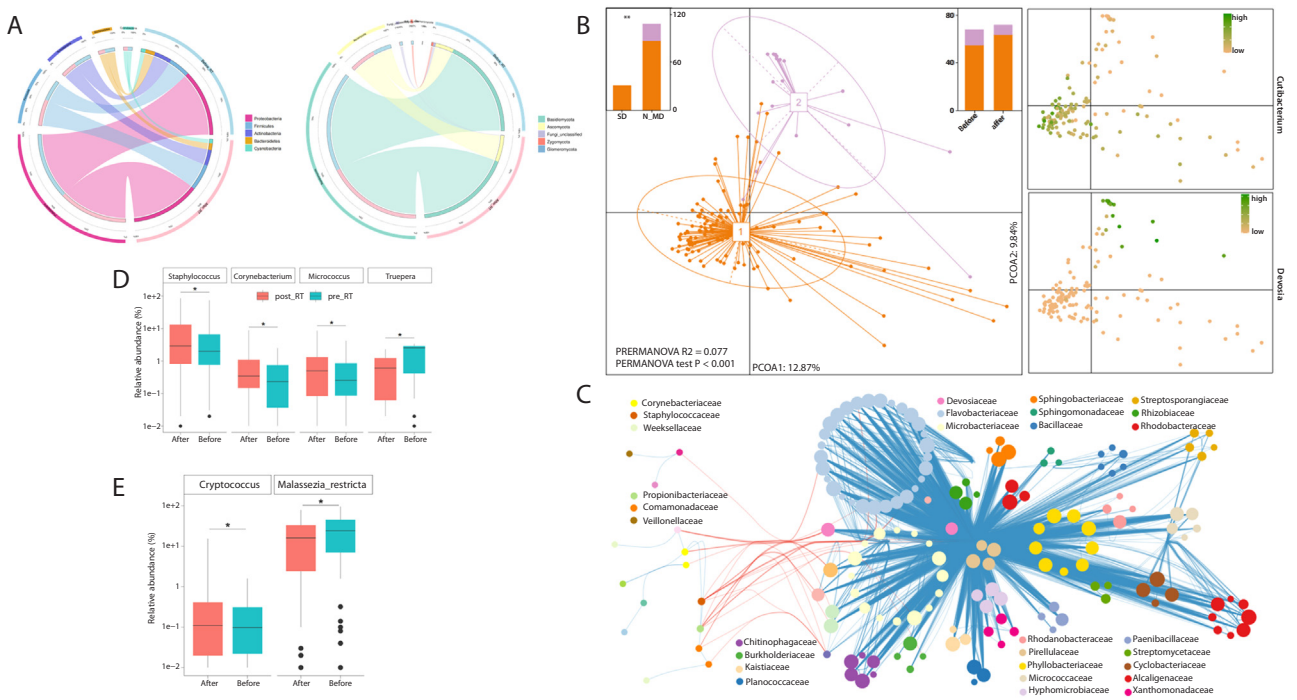

Fig. 2. Variations of skin microbiota over the course of radiation therapy (RT) in patients with breast cancer (BC). (A) Composition of common bacteria (left) and fungi (right) at the phylum level in samples from patients before RT and after RT. (B) Left: principal coordinate analysis (PCoA) using Jensen−Shannon dissimilarity presenting the clustering of 140 samples based on fungi and bacteria from patients with BC undergoing RT after reconstructive surgery. Boxplot in the top left showed the association of the dermotypes with the severity of acute radiation dermatitis (ARD). C-dermotype (orange, N = 119): SD = 31, N_MD = 88; D-dermotype (purple, N = 21): SD = 0, N_MD = 21. Boxplot in the top right showed no significant shift in dermotypes between samples before and after RT. Right: relative abundances of the 2 species: *Cutibacterium* (upper) and *Devosiaceae* (lower). (C) Coccurrence networks of the 2 dermotypes. Species enriched in the C-dermotype are shown on the left side, whereas species enriched in the D-dermotype are shown on the right side. Boxplot showing the relative abundances of the selected differentially abundant (D) bacterial taxa and (E) fungal taxa before RT (blue) and after RT (orange) analyzed by linear discriminant analysis (LDA) effect size (LefSe) (Kruskal−Wallis test, $P < .05$, LDA score > 3). Pre_RT: samples from treated sides before RT; Post_RT: samples from treated sides after RT.

on the dominance of 1 of the 2 species: *Cutibacterium* (C-dermotype) and *Devosiaceae* (D-dermotype). The dermotypes in 82.3% of the patients remained unchanged after RT, indicating their relative stability. The D-dermotype was composed entirely of N_MD, whereas the C-dermotype was composed of a mixture of N_MD and SD ($P < .01$) (Fig. 2B). Differential analysis revealed that the microbes preferentially appeared within each dermotype. For example, *Corynebacteriaceae* and *Staphyloccaceae* were enriched in the C-dermotype, whereas the D-dermotype was highly diversified, with several signature genera including *Burkholderiaceae* and *Flavobacteriaceae* enriched (Fig. 2C). Furthermore, bacteria associated with the 2 skin types displayed a significant positive correlation within each type, whereas a notable negative correlation was observed between the 2 skin types (Fig. 2B). This suggests the existence of stable microbial ecological networks within each skin type and potential antagonistic interactions between the different skin types.

Despite the relative stability of dermotypes and the overall structure of the skin microbiota before and after RT, taxonomic analyses of bacteria and fungi using LEfSe revealed a couple of differentially abundant genera after RT (Table E1). Notably, *Staphylococcus, Corynebacterium*, and *Micrococcus* genera increased following RT, and *Truepera* significantly decreased following RT (Fig. 2D). An increase in *Corynebacterium* and *Micrococcus* genera and a decrease in *Truepera* genus after RT were found exclusively in N_MD (Fig. E1E, G). In taxonomic analyses of fungi, LEfSe results revealed that *Cryptococcus* genus increased following RT (Fig. 2E), which was found exclusively in N_MD (Fig. E1F, H), and *Malassezia restricta* significantly decreased following RT (Fig. 2E).

The microbiota network revealed that most interactions between the genera were positive or symbiotic. *Staphylococcus, Cutibacterium*, and *Corynebacterium*, which were potentially "pathogenic bacteria" as we will discuss in the next part, are involved in more positive or symbiotic interactions after RT than at baseline. On the contrary, *Ralsonia* and *Methyloversatilis,* which were potentially "protective bacteria" as mentioned in the next part, were involved in more negative or antagonistic interactions after RT than at baseline (Fig. E2A, B). Together, these results suggest that RT may perturb the interactions of several skin microbiota despite the relative stability of the dermotypes over the course of RT.

Multi-kingdom skin microbiota correlated with the severity of ARD in patients with BC undergoing RT after reconstructive surgery

We speculated that skin microbiota is associated with ARD. To test this hypothesis, we conducted a cross-sectional comparison between SD and N_MD. In our analysis, 16S rRNA samples in N_MD demonstrated significantly higher bacterial richness (observed otus) and a trend toward higher diversity (Shannon) than in SD (Fig. 3A, B). In addition, ITS samples in SD both before and after RT demonstrated significantly higher fungal diversity (Shannon) than those in N_MD, with similar fungal richness (observed otus) between the 2 groups (Fig. 3E, F). PCoA based on Bray −Curtis dissimilarity metrics showed some but not dramatic differences between SD and N_MD (Fig. 3C, D, G, and H).

We analyzed the multi-kingdom skin microbiota to explore discriminatory taxa as biomarkers. As shown by LEfSe of bacteria, *Staphylococcus* and *Corynebacterium* genera both before and after RT, in addition to *Cutibacterium* genus before RT were significantly enriched in SD, whereas several bacterial taxa in the *Bacteroidetes* phylum either before or after RT, in addition to *Ralstonia* and *Methyloversatilis* genera of *Proteobacteria* phylum were significantly enriched in N_MD (Fig. 4A, C; Table E1). In addition, as demonstrated by the LEfSe of fungi, a couple of fungal taxa were significantly enriched in SD, including species in *Malassezia* genera both before and after RT, in addition to *Sporidiobolus* and *Davidiella* genera before RT, whereas *Aspergillus vitricola* before RT and *Trichosporon* genus after RT were significantly enriched in N_MD (Fig. 4B, D; Table E1). Next, PICRUSt2 was used to assess functional differences by plotting differential pathways against the MetaCyc database. Several anabolic functions, including fatty acid and amino acid biosynthesis, were predicted to be more enriched in N_MD than in SD at the baseline (Fig. E3), which may promote host immunity.[2] In contrast, more anabolic functions, including nucleotide biosynthesis, were predominant in SD, whereas several catabolic functions, including sugar and myo-inositol degradation, were predominant in N_MD (Fig. E4) after RT, which may reflect the microbial response to radiation damage.[24]

Differences in the severity of ARD were also reflected in the microbiota networks of skin microbiota samples (Fig. E2C-F). More interactions were identified in N_MD than in SD both before and after RT, which reflects the contribution of both synergistic and antagonistic interactions to skin microbiota homeostasis and suggests that some specific ecological interactions may help alleviate the severity of ARD. In particular, potentially "pathogenic bacteria and fungi" (*Staphylococcus, Corynebacterium, Cutibacterium*, and *Malassezia*) were identified to be involved in a significant negative or antagonistic relationship with potentially "protective bacteria and fungi" (*Ralsonia, Methyloversatilis*, and *Aspergillus*), a phenomenon that is more notable in N_MD than in SD (Fig. E2C-F). In addition, the interactions formed with potentially "protective bacteria and fungi" were found to be more stable in N_MD than in SD. For example, the synergistic interactions of "protective fungus" *Aspergillus* with a couple of other bacteria were disrupted after RT in SD whereas in N_MD, the antagonistic interaction of *Aspergillus* with potentially "pathogenic fungi" *Malassezia* maintained after RT (Fig. E2C-F). The differences in microbiota networks between N_MD and SD reflect the importance of co-occurrence ecological interactions in skin microbiota homeostasis.

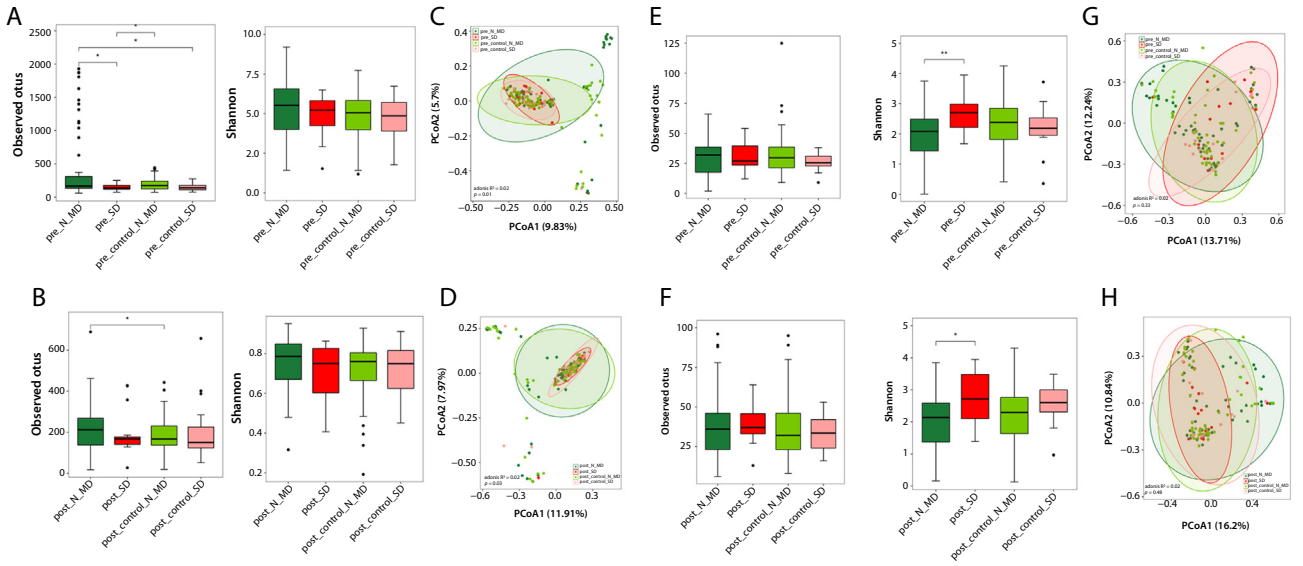

Fig. 3. Diversity of skin microbiota correlated with the severity of acute radiation dermatitis (ARD) in patients with breast cancer (BC) undergoing radiation therapy (RT) after reconstructive surgery. Comparison of bacterial richness (observed otus, left panel) and diversity (Shannon index, right panel) by Mann−Whitney test before (A) and after (B) RT between N_MD and SD patients in both the treated and contralateral healthy sides. Principal coordinate analysis (PCoA) by the degree of dermatitis using Bray−Curtis distance of bacterial communities before (C) and after (D) RT in both the treated and contralateral healthy sides. Comparison of fungal richness (observed otus, left panel) and diversity (Shannon index, right panel) by Mann−Whitney test before (E) and after (F) RT between N_MD and SD patients in both the treated and contralateral healthy sides. PCoA by the degree of dermatitis using Bray−Curtis distance of fungal communities before (G) and after (H) RT in both the treated and contralateral healthy sides. *$P < .05$. Pre_N_MD or pre_control_N_MD: samples from treated or contralateral healthy sides in no or mild ARD subgroup (RTOG grade 0-1) before RT; pre_SD or pre_control_SD: samples from treated or contralateral healthy sides in significant ARD subgroup (RTOG grade≥2) before RT; post_N_MD or post_control_N_MD: samples from treated or contralateral healthy sides in no or mild ARD subgroup (RTOG grade 0-1) after RT; post_SD or post_control_SD: samples from treated or contralateral healthy sides in significant ARD subgroup (RTOG grade≥2) after RT.

The establishment of a predictive dermatitis classifier

In this study, we employed random forest analysis to develop 3 distinct classifiers aimed at predicting ARD using microbial variables from skin samples: bacteria, fungi, and a combination of both. The training and test cohorts were randomly selected in a ratio of 8:2. The training cohort comprised 71 samples with 56 N_MD and 15 SD and the test set comprised 18 samples with 10 N_MD and 8 SD. Bacteria-based classifier I, which utilized 154 bacterial genera (Table E2), achieved an AUC of 94.64% with a confidence interval (CI) of 83.58% to 100% in the test set (Fig. 5A). This high AUC indicates a strong capability to differentiate between N_MD and SD based on bacterial profiles. In the bacterial model, *Herbaspirillum, Atopostipes, Eggerthella, Enterobacter, Acinetobacter, Corynebacterium*, and *Staphylococcus* were the primary contributors (Fig. 5D). Additionally, a significant difference in the probability of response (POR) between the N_MD and SD groups was observed ($P = .0046$; Fig. 5A), confirming the relevance of bacterial variables in ARD prediction. Fungi-based classifier II, which incorporated 10 fungal genera (Table E2), showed a lower AUC of 80%, with a CI of 56.11% to 100% in the test set (Fig. 5B). This suggests that fungal variables alone may have less predictive value for ARD compared with bacterial variables. And the difference in POR was less pronounced ($P = .1$; Fig. 5B), indicating a weaker association between fungal profiles and ARD.

Classifier III combined both bacterial and fungal variables, resulting in an AUC of 91.67% with a CI of 74.54% to 100% in the test set (Fig. 5C). In the multi-kingdom model, *Herbaspirillum, Enterobacter, Staphylococcus, Corynebacterium, Gordonia, Bionectria*, and *Capnodiales* were the primary contributors (Fig. 5F). The improved accuracy over the fungi-only model suggests a synergistic effect when both bacterial and fungal data were considered, with a statistically significant difference in POR ($P = .008$, Fig. 5C). Overall, classifiers I and III, which included bacterial variables, performed significantly better than classifier II, which relied solely on fungal variables. These results highlight the critical role of bacterial components in the skin microbiome over that of fungal components in predicting ARD. These findings also support the potential of exploring microbiome-based classifiers in dermatological research and clinical applications, highlighting the importance of comprehensive microbial analysis for enhancing the predictive accuracy of ARD.

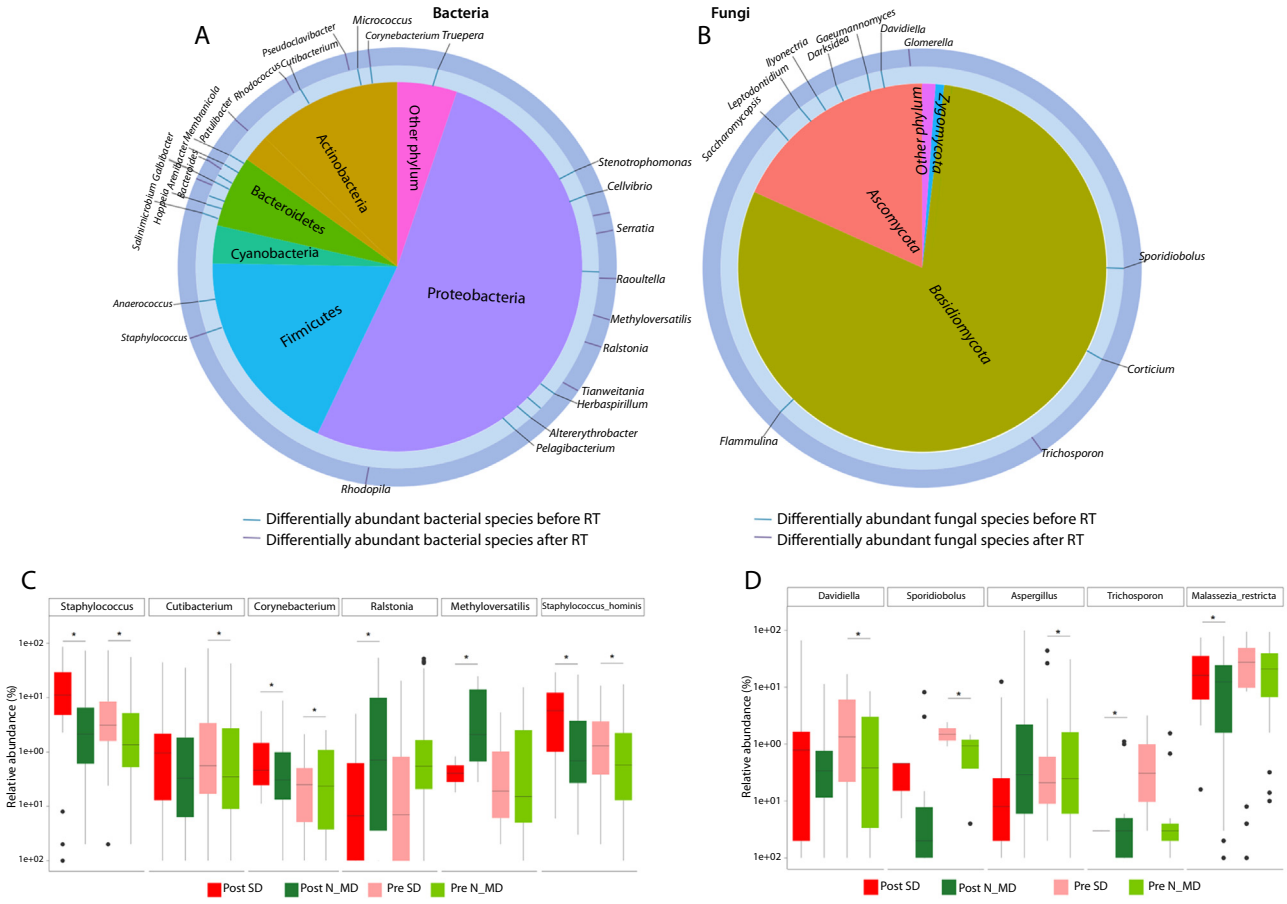

Fig. 4. Multi-kingdom skin microbiota correlated with the severity of acute radiation dermatitis (ARD) in patients with breast cancer (BC) undergoing radiation therapy (RT) after reconstructive surgery. Circular plot showing differentially abundant (A) bacterial and (B) fungal species between N_MD and SD samples detected by linear discriminant analysis (LDA) effect size (LEfSe) (Kruskal–Wallis test, $P < .05$, LDA score > 3). The differentially abundant species before RT were highlighted in the inner circle in blue, whereas differentially abundant species after RT were marked in purple in the outer circle. The phylum of these markers was indicated in the center. Boxplot showing the relative abundances of the selected differentially abundant (C) bacterial taxa and (D) fungal taxa in N_MD and SD analyzed by LefSe (Kruskal–Wallis test, $P < .05$, LDA score > 3). Pre_SD or post_SD: samples from treated sides in significant ARD subgroup (RTOG grade ≥ 2) before or after RT. Pre_N_MD or post_N_MD: samples from treated sides in no or mild ARD subgroup (RTOG grade 0-1) before or after RT.

Discussion

The pathogenesis of ARD remains unclear, which impedes the development of effective prevention and treatment strategies.[25] In this prospective, longitudinal study, we present multi-kingdom microbial biomarkers for ARD in patients with BC undergoing RT after reconstructive surgery, providing the basis for further exploration of reducing ARD by regulating skin microbiota.

Our study demonstrated the relative stability of dermotypes and the overall structure of skin microbiota before and after RT. A previous study has shown that the recovery of skin microbiota within 1 hour after cleansing and reached a certain dynamic equilibrium by 1 day.[26] Similarly, RT, as a selective pressure for microbiota taxa, may perturb skin homeostasis and achieve a dynamic balance. In this study, significant differences in the skin microbiota were identified between the N_MD and SD groups. This study confirmed the relationship between several potentially "pathogenic microbes" and ARD. The role of *Staphylococcus aureus* in the pathogenesis and recovery from ARD has been demonstrated in previous studies.[10,27] In addition, several other potentially "pathogenic microbiota" *Cutibacterium*[28] and *Malassezia* genus[29,30] were also enriched in SD. *Cutibacterium* (eg, *Cutibacterium acnes*) and *Malassezia* genus play important roles in many skin diseases.[28-31] Previous studies have elucidated the effects of RT on the skin and the immune system.[24] It is speculated that the phylotype diversity of some specific microbiota is altered after RT and that the potentially "pathogenic microbiota" may initiate or exacerbate ARD in the context of skin barrier defects or altered immunity caused by RT. In addition, several potentially "protective microbiota" have been identified in ARD. Several bacterial taxa in the *Bacteroidetes* and *Proteobacteria* phyla, including *Ralstonia* and *Methyloversatilis* genera in addition to *Aspergillus* and *Trichosporon* were enriched in

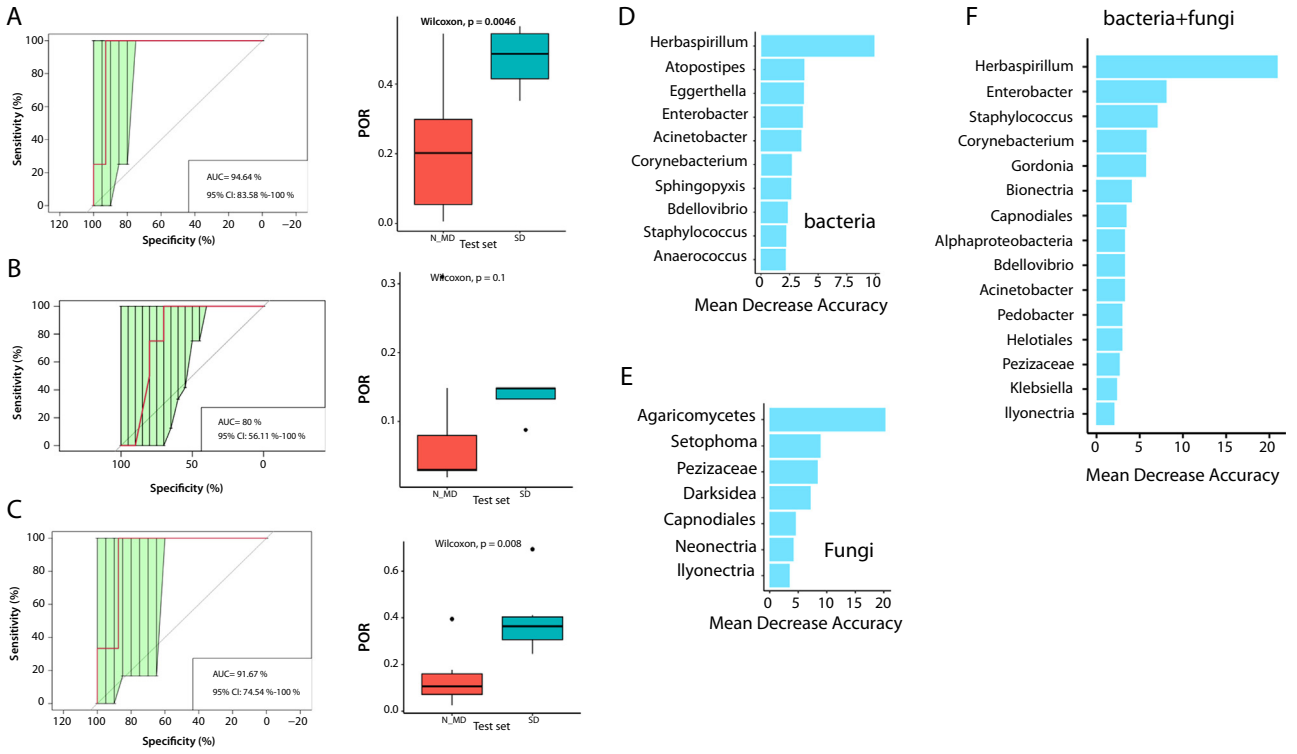

Fig. 5. The establishment of a predictive classifier for acute radiation dermatitis (ARD) based on the skin microbiome. (A) The predictive classifier based on the random forest classifier was constructed by bacterial variables only. Left panel: the receiver operating characteristic curve (ROC) for the test set. The area under the ROC curve (AUC) was 94.64% (95% CI, 83.58%-100%). Right panel: boxplot for the probability of response (POR) in the test set was $P = .0046$. (B) The predictive classifier based on the random forest classifier was constructed by fungal variables only. Left panel: the ROC for the test set. The AUC was 80% (95% CI, 56.11%-100%). Right panel: boxplot for the POR in the test set was $P = .1$. (C) The predictive classifier based on the random forest classifier was constructed by both bacterial and fungal variables. Left panel: the ROC for the test set. The AUC was 91.67% (95% CI, 74.54%-100%). Right panel: boxplot for the POR in the test set was $P = .008$. Selected microbial variables from random forest model based on (D) bacteria, (E) fungi, and (F) multi-kingdom microbiota, ranked by importance as assessed by their corresponding contributions to the mean decrease accuracy.

N_MD. "Favorable microbiota" may alleviate ARD by influencing immune responses; however, the detailed mechanisms require further investigation.

Although it is important to understand the impact of individual microbes on the skin, a complete microbial community has unique and pronounced effects on skin.[32] In this study, the D-dermotype was identified as a potentially protective dermotype. Notably, RT did not significantly change the dermotype of the patients, which was largely because of the stable ecological networks formed by the interrelated skin microbiota within 1 dermotype. Additionally, the skin microbiota-based random forest classifiers (I and III) robustly discriminated between SD and N_MD. The results verified the importance of the full and diverse community of multi-kingdom skin microbiota in the pathogenesis of ARD in patients with BC undergoing RT after reconstructive surgery.

To date, 2 clinical trials have investigated preventive approaches utilizing microbial decolonization as a strategy. The clinical trial by Kost et al[11] demonstrated the efficacy of bacterial decolonization using intranasal mupirocin ointment and chlorhexidine body cleanser for ARD prophylaxis. Another approach involves the topical application of noninvasive physical plasma (NIPP), a well-tolerated, partially ionized gas generated from ambient air and characterized by free electrons. NIPP has shown potential benefits in ARD prevention in BC and its primary mechanism of action may involve reducing the bacterial load on the irradiated skin.[12] Our study identified potentially protective microbiota and dermotypes associated with reduced ARD incidence and severity, in addition to pathogenic microbes and dermotypes. Beyond targeting harmful bacteria, future strategies could focus on enhancing the skin's microecological balance to promote the colonization of protective bacteria, thereby shifting the dermotype toward a more protective state and ultimately preventing ARD.

Our study had some limitations. One limitation was the utilization of 16S rRNA and ITS sequencing, which had a lower taxonomic resolution and limited ability to identify microbial functions compared with shotgun sequencing. Moreover, skin microbiota was collected and analyzed at only 2 time points (pre- and post-RT), which may not fully capture the dynamic and evolving changes in the skin

microbiome during radiation therapy.[9] Additionally, potential confounding factors for ARD such as the biophysical parameters of skin (eg, transepidermal water loss, skin hydration, and skin pH) and the nasal *S. aureus* colonization[10] were not measured. Despite these limitations, our study obtained meaningful results that warrant validation in future research.

In summary, this longitudinal, prospective study revealed the association of multi-kingdom skin microbiota with ARD in patients with BC undergoing RT after reconstructive surgery. With the identification of a protective dermotype and robust discrimination power using the dermatitis-prediction random forest classifier, our results have important implications for the prevention and treatment of ARD in patients with BC.

References

1. Chen YE, Fischbach MA, Belkaid Y. Skin microbiota-host interactions. *Nature* 2018;553:427-436.
2. Byrd AL, Belkaid Y, Segre JA. The human skin microbiome. *Nat Rev Microbiol* 2018;16:143-155.
3. Rzepecki A, Birnbaum M, Ohri N, et al. Characterizing the effects of radiation dermatitis on quality of life: A prospective survey-based study. *J Am Acad Dermatol* 2022;86:161-163.
4. Delfino S, Brunetti B, Toto V, Persichetti P. Burn after breast reconstruction. *Burns* 2008;34:873-877.
5. Zugasti A, Hontanilla B. The impact of adjuvant radiotherapy on immediate implant-based breast reconstruction surgical and satisfaction outcomes: A systematic review and meta-analysis. *Plast Reconstr Surg Glob Open* 2021;9:e3910.
6. Behroozian T, Bonomo P, Patel P, et al. Multinational Association of Supportive Care in Cancer (MASCC) clinical practice guidelines for the prevention and management of acute radiation dermatitis: International Delphi consensus-based recommendations. *Lancet Oncol* 2023;24:e172-e185.
7. Ramadan M, Hetta HF, Saleh MM, Ali ME, Ahmed AA, Salah M. Alterations in skin microbiome mediated by radiotherapy and their potential roles in the prognosis of radiotherapy-induced dermatitis: A pilot study. *Sci Rep* 2021;11:5179.
8. Huang B, An L, Su W, Yan T, Zhang H, Yu DJ. Exploring the alterations and function of skin microbiome mediated by ionizing radiation injury. *Front Cell Infect Microbiol* 2022;12:1029592.
9. Hülpüsch C, Neumann AU, Reiger M, et al. Association of skin microbiome dynamics with radiodermatitis in patients with breast cancer. *JAMA Oncol* 2024;10:516-521.
10. Kost Y, Rzepecki AK, Deutsch A, et al. Association of *Staphylococcus aureus* colonization with severity of acute radiation dermatitis in patients with breast or head and neck cancer. *JAMA Oncol* 2023;9:962-965.
11. Kost Y, Deutsch A, Mieczkowska K, et al. Bacterial decolonization for prevention of radiation dermatitis: A randomized clinical trial. *JAMA Oncol* 2023;9:940-945.
12. Dejonckheere CS, Layer JP, Nour Y, et al. Non-invasive physical plasma for preventing radiation dermatitis in breast cancer: Results from an intrapatient-randomised double-blind placebo-controlled trial. *Clin Transl Radiat Oncol* 2024;44:100699.
13. Porock D, Kristjanson L. Skin reactions during radiotherapy for breast cancer: The use and impact of topical agents and dressings. *Eur J Cancer Care (Engl)* 1999;8:143-153.
14. Martin M. *Cutadapt removes adapter sequences from high-throughput sequencing reads* 2011;17:3.
15. Magoč T, Salzberg SL. FLASH: Fast length adjustment of short reads to improve genome assemblies. *Bioinformatics* 2011;27:2957-2963.
16. Segata N, Izard J, Waldron L, et al. Metagenomic biomarker discovery and explanation. *Genome Biol* 2011;12:R60.
17. Douglas GM, Maffei VJ, Zaneveld JR, et al. PICRUSt2 for prediction of metagenome functions. *Nat Biotechnol* 2020;38:685-688.
18. Caspi R, Billington R, Keseler IM, et al. The MetaCyc database of metabolic pathways and enzymes - A 2019 update. *Nucleic Acids Res* 2020;48:D445-D453.
19. Li Z, Xia J, Jiang L, et al. Characterization of the human skin resistome and identification of two microbiota cutotypes. *Microbiome* 2021;9:47.
20. Maechler M, Rousseeuw P, Struyf A, Hubert M, Hornik K. (2025). cluster: Cluster Analysis Basics and Extensions. R package version 2.1.8.1 — For new features, see the 'NEWS' and the 'Changelog' file in the package source), Available at: https://CRAN.R-project.org/package=cluster.
21. Dixon P. VEGAN, a package of R functions for community ecology. *J Vegetation Sci* 2003;14:927-930.
22. Liaw A, Wiener M. Classification and Regression by Random Forest. *R News* 2002;2(3):18-22.
23. K.M. Zielinska-Dabkowska: D. Vitamin, The truth about Vitamin D and sun exposure demystified. Finding the balance for personal health, *Professional Lighting Design*, May 40-48, 2014. Available at: https://www.researchgate.net/figure/Skin-type-and-tanning-ability-based-on-the-Fitzpatrick-skin-pigmentation-scale_tbl1_285056396. Accessed April 26, 2025.
24. Kumari S, Mukherjee S, Sinha D, Abdisalaam S, Krishnan S, Asaithamby A. Immunomodulatory effects of radiotherapy. *Int J Mol Sci* 2020;21:8151.
25. Rosenthal A, Israilevich R, Moy R. Management of acute radiation dermatitis: A review of the literature and proposal for treatment algorithm. *J Am Acad Dermatol* 2019;81:558-567.
26. Sfriso R, Claypool J. Microbial reference frames reveal distinct shifts in the skin microbiota after cleansing. *Microorganisms* 2020;8:1-16.
27. Buda A, Międzobrodzki J. The role of *Staphylococcus aureus* in secondary infections in patients with atopic dermatitis (AD). *Pol J Microbiol* 2016;65:253-259.
28. Mias C, Mengeaud V, Bessou-Touya S, Duplan H. Recent advances in understanding inflammatory acne: Deciphering the relationship between *Cutibacterium acnes* and Th17 inflammatory pathway. *J Eur Acad Dermatol Venereol* 2023;37:3-11.
29. Carmona-Cruz S, Orozco-Covarrubias L, Sáez-de-Ocariz M. The human skin microbiome in selected cutaneous diseases. *Front Cell Infect Microbiol* 2022;12:834135.
30. Kurniadi I, Hendra Wijaya W, Timotius KH. Malassezia virulence factors and their role in dermatological disorders. *Acta Dermatovenerol Alp Pannonica Adriat* 2022;31:65-70.
31. Yu T, Xu X, Liu Y, et al. Multi-omics signatures reveal genomic and functional heterogeneity of *Cutibacterium acnes* in normal and diseased skin. *Cell Host Microbe* 2024;32:1129-1146.
32. Loomis KH, Wu SK, Ernlund A, et al. A mixed community of skin microbiome representatives influences cutaneous processes more than individual members. *Microbiome* 2021;9:22.